Theoretical and Kinetic Assessment of the Mechanism of Ethane Hydrogenolysis on Metal Surfaces Saturated with Chemisorbed Hydrogen

"David W. Flaherty[a,b,#], David D. Hibbitts[a,#], Elif I. Gürbüz[a], Enrique Iglesia[a,*]"

[a] *Department of Chemical Engineering, University of California at Berkeley, Berkeley, CA 94720, United States*

[b] *Department of Chemical and Biomolecular Engineering, University of Illinois at Urbana-Champaign, Urbana, IL 61801, United States*

[#] These authors contributed equally to this work.

Supporting Information

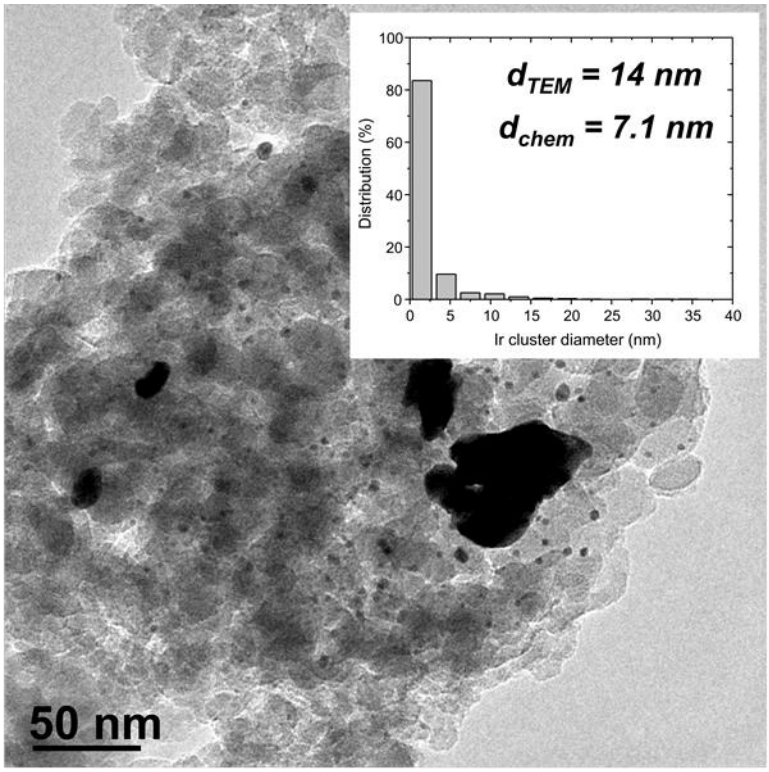

Figure S1. Representative image and particle size distribution of 7.1 nm Ir-SiO_2 as obtained by transmission electron microscopy. A total of 1,029 clusters were counted to determine d_{TEM}, the surface-averaged diameter. The sample contains a broad range of cluster sizes, however, the largest clusters dominate the value of the surface-averaged diameter.

Table S1. Summary of the synthesis conditions and characterization results for the Ir catalyst.

TEA:Ir[1]	Ir content (% wt.)	Temperature (K)		Dispersion (%)			$<d_{chem}>$ (nm) [7]	$<d_{TEM}>$ (nm) [8]
		Oxidative Treatment [2]	Reductive Treatment [3]	H_2 [4]	O_2 [5]	CO [6]		
10	3.0	1123, 12 h	1173, 8 h	13	15	13	7.1	14.4

(1) Ratio of triethanol amine to H_2IrCl_6 in aqueous solution used for SiO_2 impregnation

(2) 21 kPa O_2 (dry air)

(3) 50 kPa H_2 (balance He)

(4) H_2 chemisorption (irreversible at 300 K), assuming H:Ir = 1

(5) O_2 chemisorption (irreversible at 300 K), assuming O:Ir = 1

(6) CO chemisorption (irreversible at 300 K), assuming CO:Ir = 1

(7) Mean particle diameters, d_{chem}, calculated from $d_{chem}=C/D$, where C is 0.99 for spherical iridium particles and D is the measured dispersion from irreversible H_2 uptakes.

(8) Surface-averaged mean Ir particle diameter from TEM analysis using $<d_{TEM}> = \sum n_i d_i^3 / \sum n_i d_i^2$

Details of Density Functional Calculations of Thermochemical Properties

The enthalpy of a given state can be written as the sum of the DFT-derived energy (E_0), zero-point vibrational enthalpy (*ZPVE*) and vibrational, translational and rotational enthalpy (H_{vib}, H_{trans} and H_{rot}):

$$H = E_0 + ZPVE + H_{vib} + H_{trans} + H_{rot} \tag{S4}$$

similarly, the free energy of a state can be written as:

$$G = E_0 + ZPVE + G_{vib} + G_{trans} + G_{rot} \tag{S5}$$

and entropy can be determined for a state with a known H and G at a given T:

$$S = \frac{H - G}{T} \tag{S3}$$

For calculations which include a periodic Ir(111) surface (including adsorbed species and transition states on that surface), there are no translational or rotational degrees of freedom and DFT-derived vibrational frequencies can be used to determine the *ZPVE*, H_{vib} and G_{vib} shown in Eqns. S6-8.

$$ZPVE = \sum_i (½ \nu_i h) \tag{S6}$$

$$H_{vib} = \sum_i \left(\frac{\nu_i h e^{\frac{-\nu_i h}{kT}}}{1 - e^{\frac{-\nu_i h}{kT}}} \right) \tag{S7}$$

$$G_{vib} = \sum_i \left(-kT \ln \frac{1}{1 - e^{\frac{-\nu_i h}{kT}}} \right) \tag{S8}$$

Gas-phase molecules have translational and rotational degrees of freedom; thus H_{trans}, H_{rot}, G_{trans} and G_{rot} must also be computed: [1]

$$H_{trans} = {}^{5}/_{2}\, kT \tag{S9}$$

$$H_{rot,linear} = kT \tag{S10}$$

$$H_{rot,nonlinear} = {}^{3}/_{2}\, kT \tag{S11}$$

$$G_{trans} = -kT \ln\left[\left(\frac{2\pi MkT}{h^2}\right)^{3/2} V\right] \tag{S12}$$

$$G_{rot} = -kT \ln\left[\frac{\pi^{1/2}}{\sigma}\left(\frac{T^3}{\theta_x\theta_y\theta_z}\right)^{1/2}\right] \tag{S13}$$

$$\theta_i = \frac{h^2}{8\pi^2 I_i k} \tag{S14}$$

where I_i is the moment of inertia about axes x, y or z and σ is the symmetry number of the molecule, 2 for H_2, 12 for CH_4 and 6 for C_2H_6.

[1] Statistical Mechanics", D. A. McQuarrie, 2000, University Science Books, Sausolito, CA.

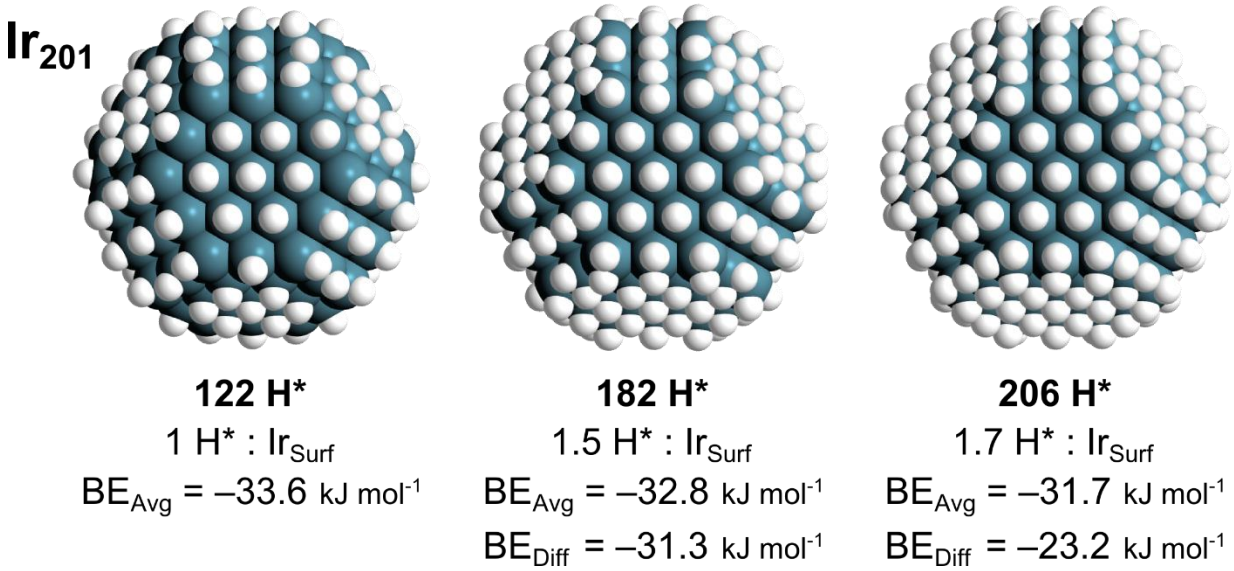

Figure S2. Binding energies of H* at different coverages on Ir_{201} model clusters. BE_{Avg} indicates the average of all H* atoms on the surface whereas BE_{Diff} indicates the average change in BE that results from adding the indicated number of H*-atoms to the surface with lower coverage.

Figure S2 shows that the binding energy (BE) of H*-atoms on Ir_{201} particles does not significantly decrease at coverages greater than 1 H*:Ir_s, indicating that some Ir_s atoms will have > 1 H*-atoms at high H_2 pressures. For instance, increasing the H*-atom coverage from 122 H* (1 H*:Ir_s) to 182 H* (1.5 H*:Ir_s) by the addition of 60 H* atoms at under-saturated corners and edges, only decreases the average BE of the 60 added H* atoms (BE_{Diff}) to -31.3 kJ mol^{-1} from the average BE of the 122 original H*-atoms (-33.6 kJ mol^{-1}). Similarly, the addition of 24 H* to the 182 H*-atom model to generate a model with 206 H* atoms (1.7 H*:Ir_s), decreases the BE_{Diff} to -23 kJ mol^{-1}.

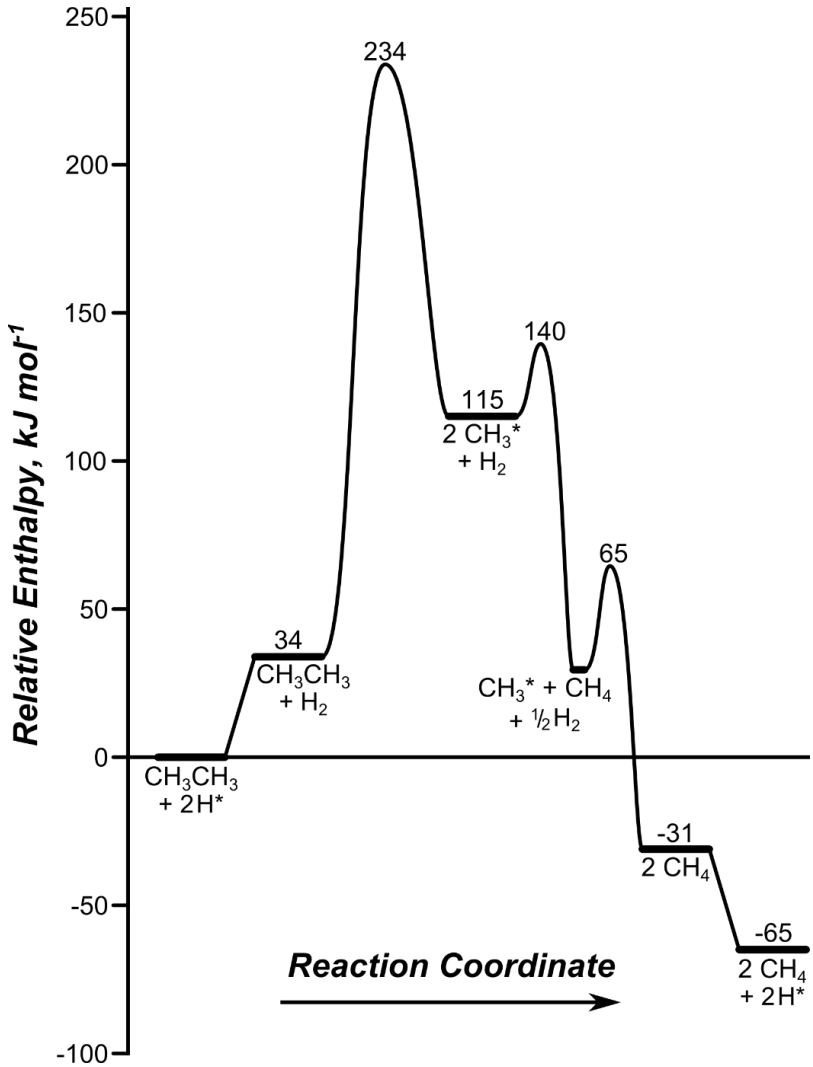

Figure S3. Reaction coordinate diagram for ethane hydrogenolysis via C-C bond rupture in CH_3CH_3*.

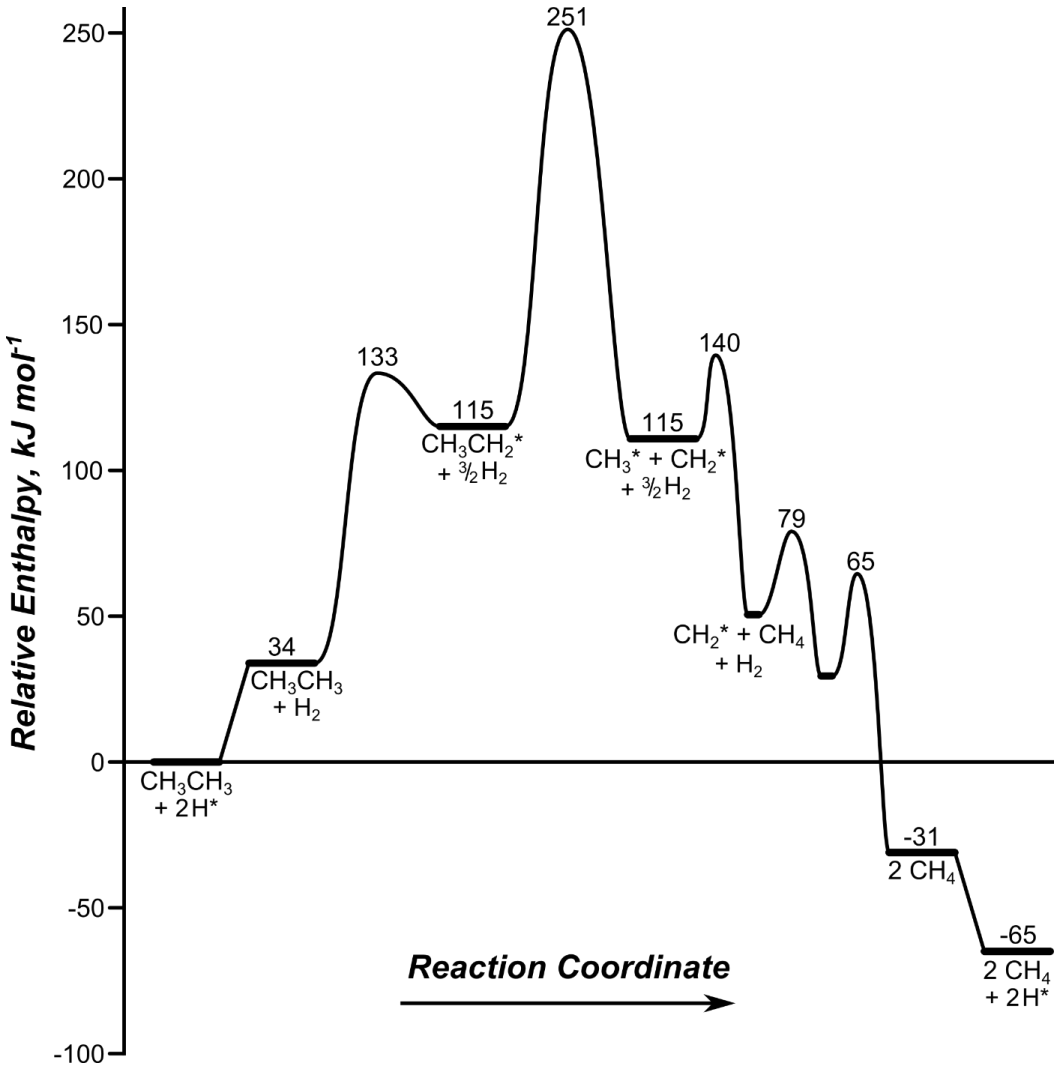

Figure S4. Reaction coordinate diagram for ethane hydrogenolysis via C-C bond rupture in CH_3CH_2*.

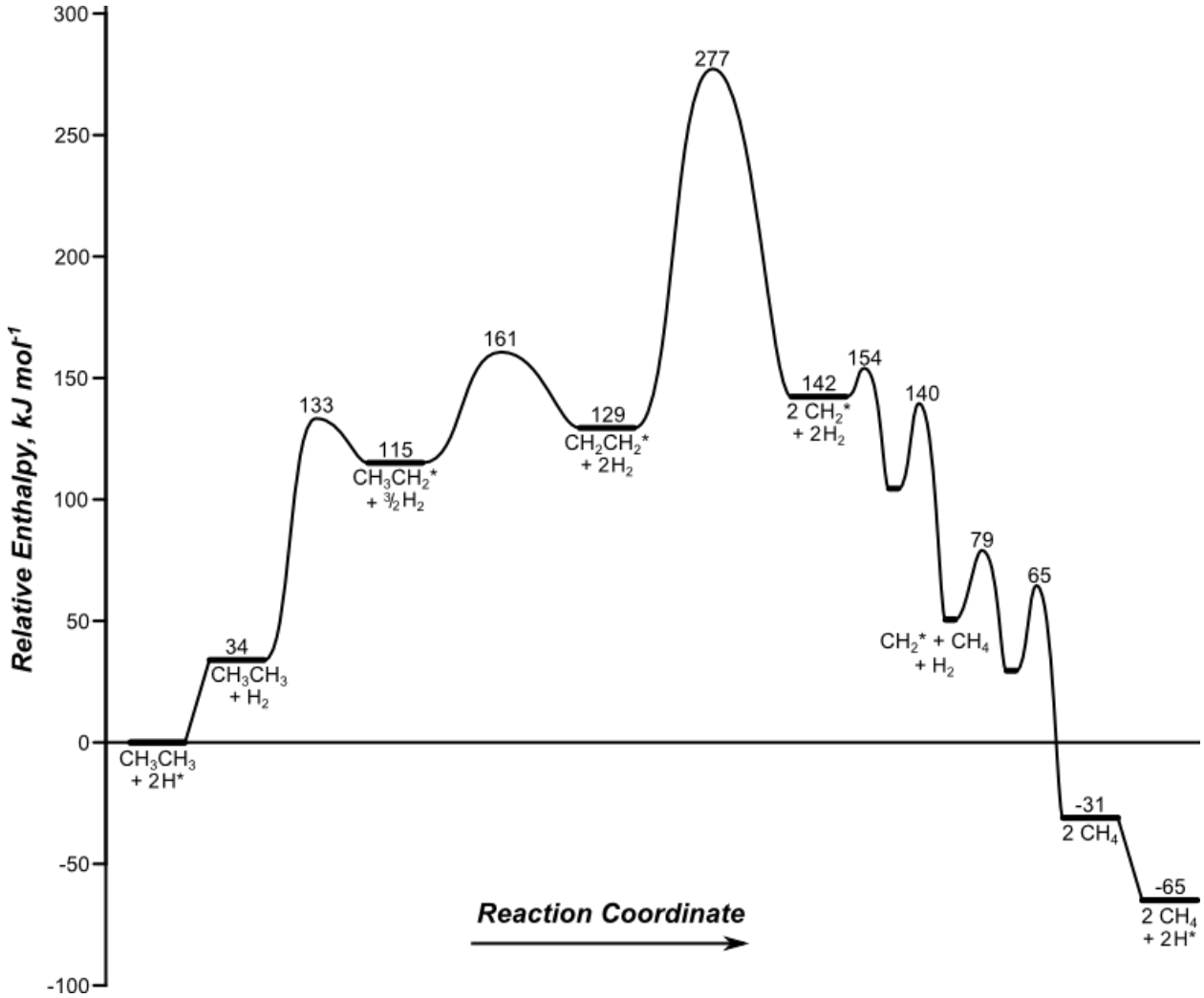

Figure S5. Reaction coordinate diagram for ethane hydrogenolysis via C-C bond rupture in $*CH_2CH_2*$.

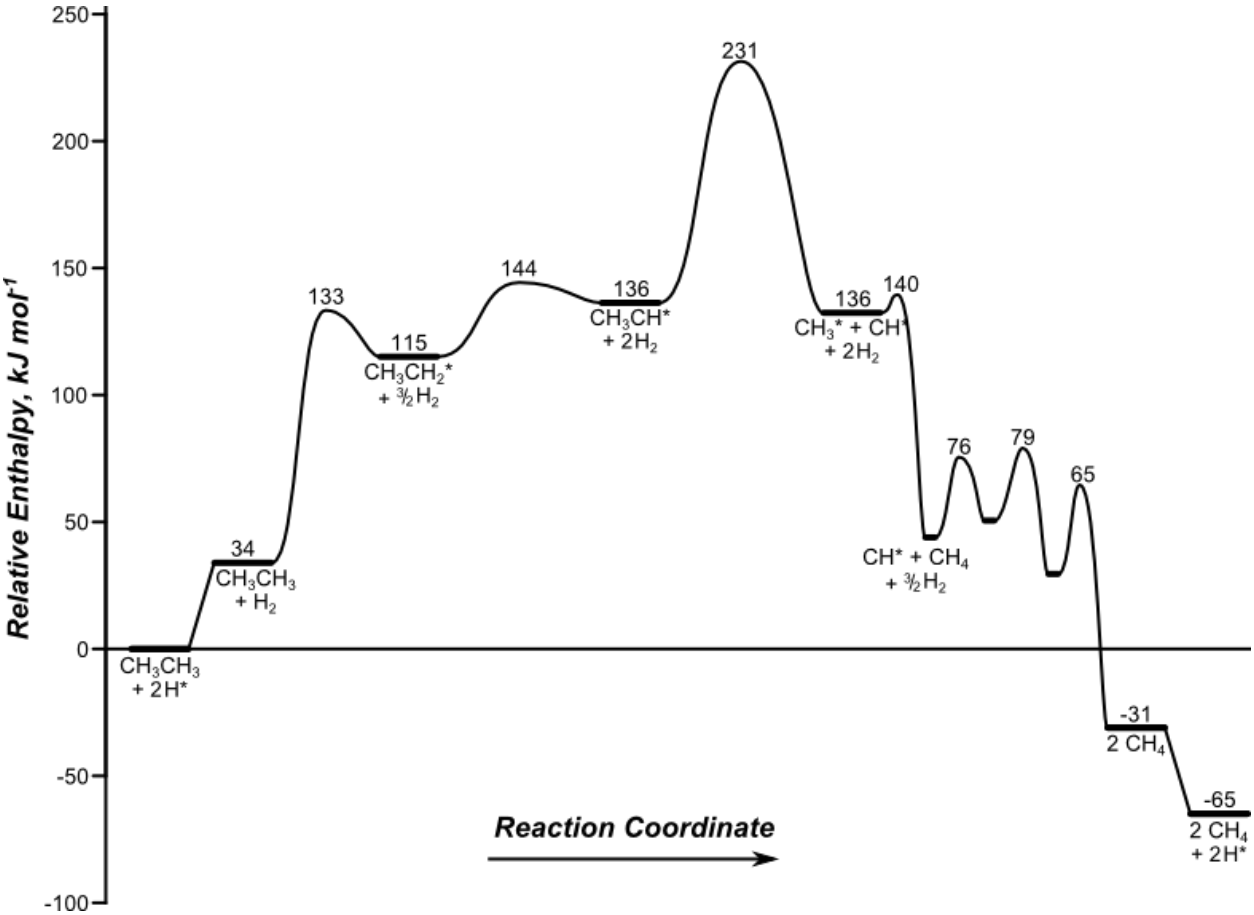

Figure S6. Reaction coordinate diagram for ethane hydrogenolysis via C-C bond rupture in $*CH_3CH*$.

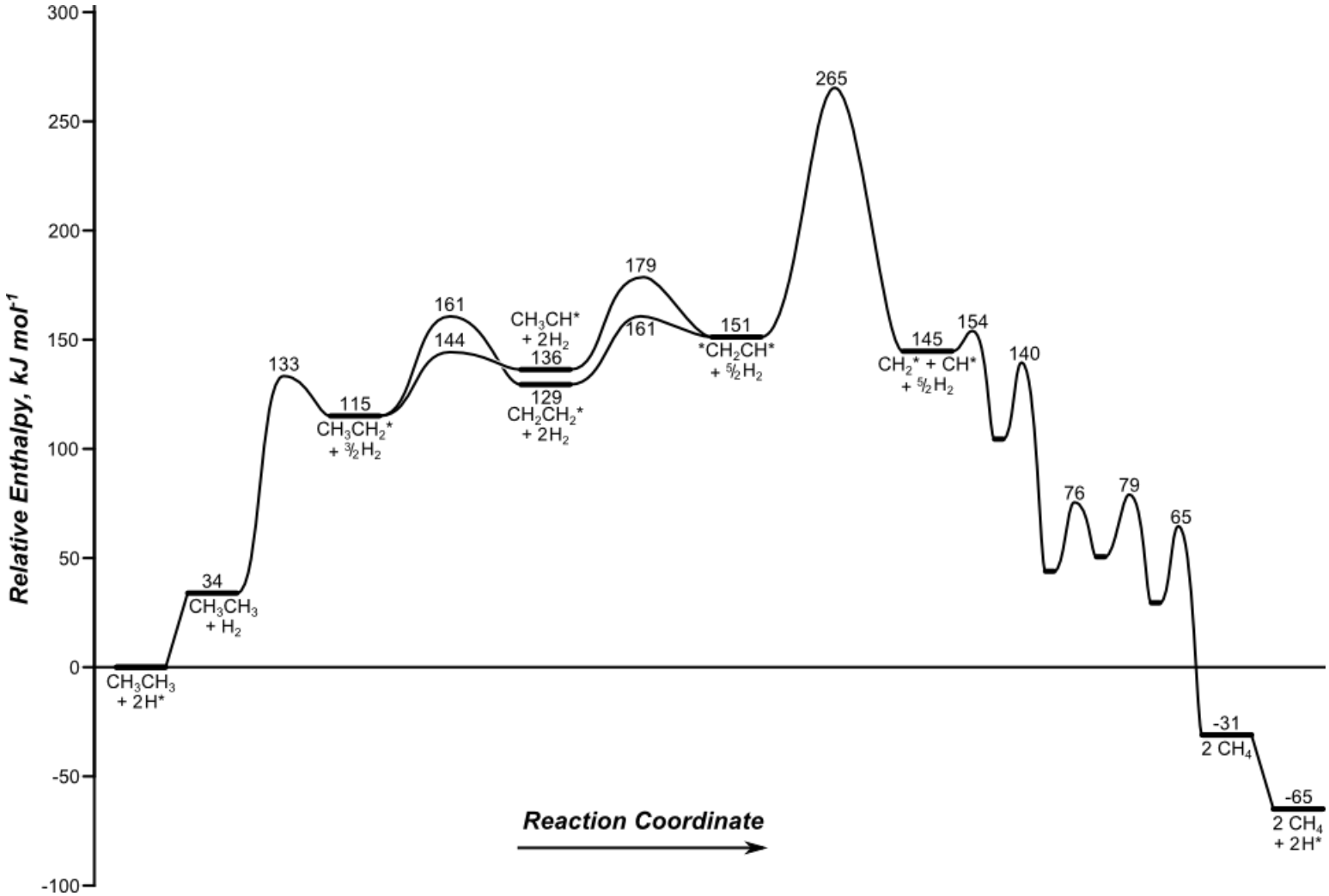

Figure S7. Reaction coordinate diagram for ethane hydrogenolysis via C-C bond rupture in $*CH_2CH*$.

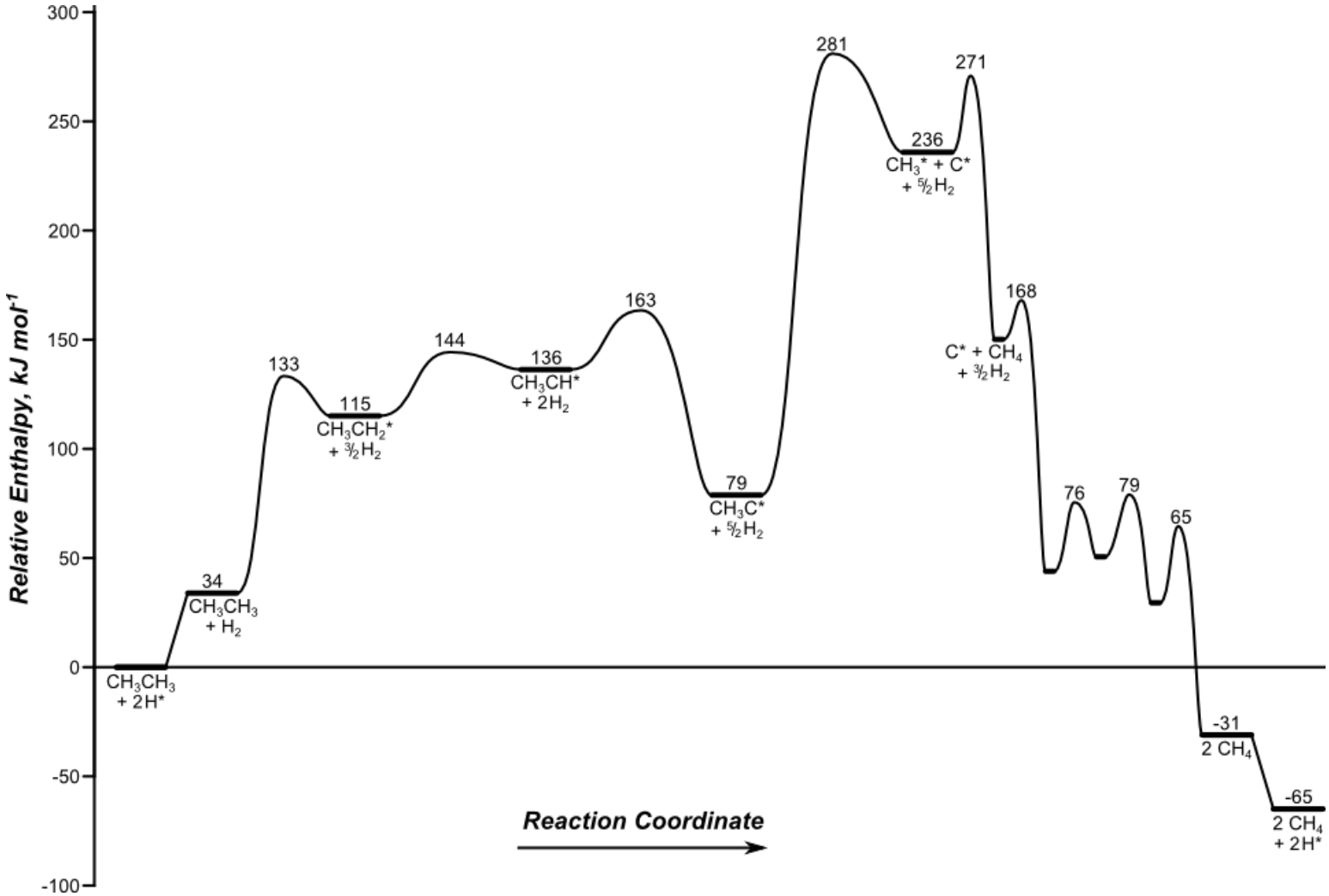

Figure S8. Reaction coordinate diagram for ethane hydrogenolysis via C-C bond rupture in *CH_3C*.

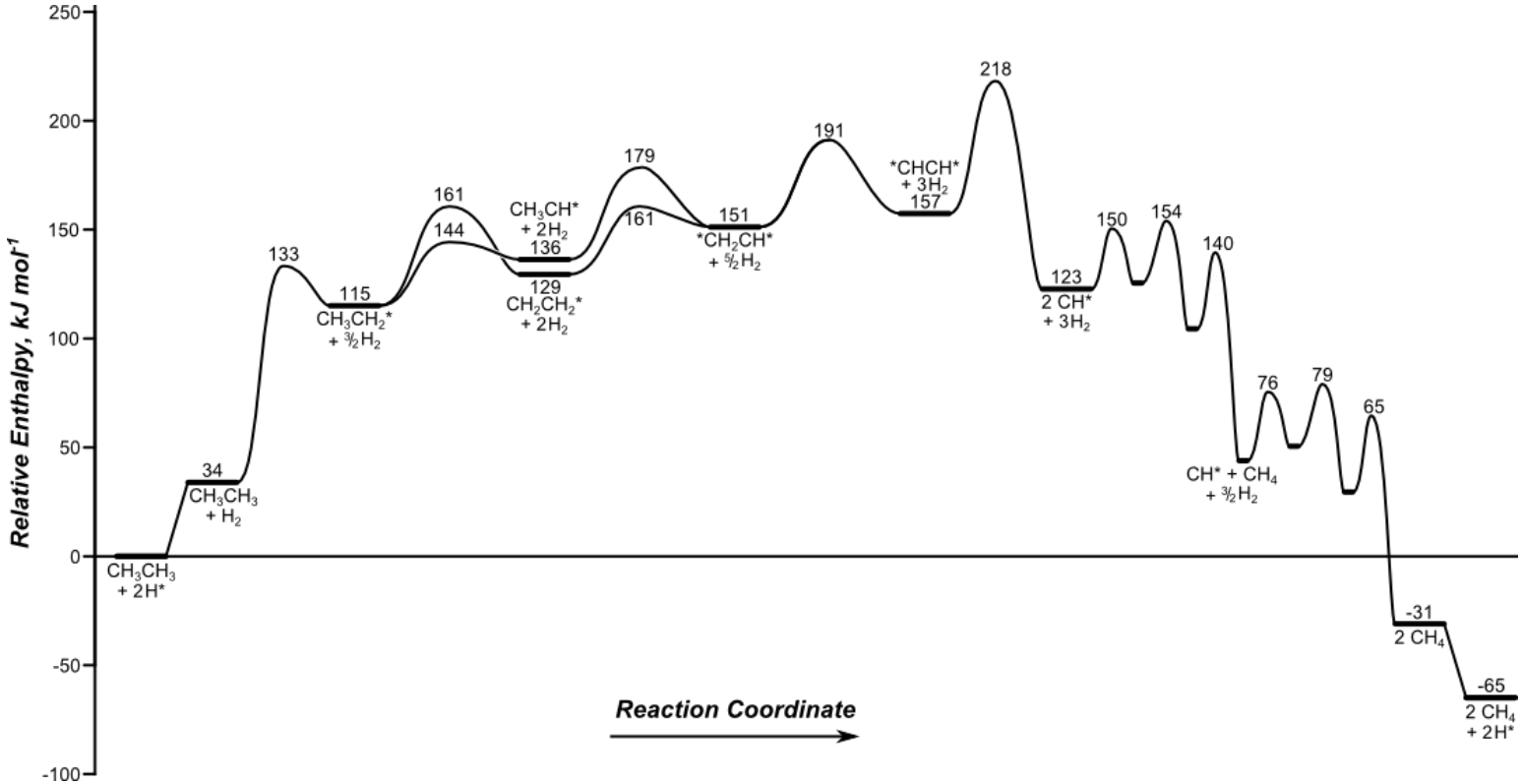

Figure S9. Reaction coordinate diagram for ethane hydrogenolysis via C-C bond rupture in *CHCH*.

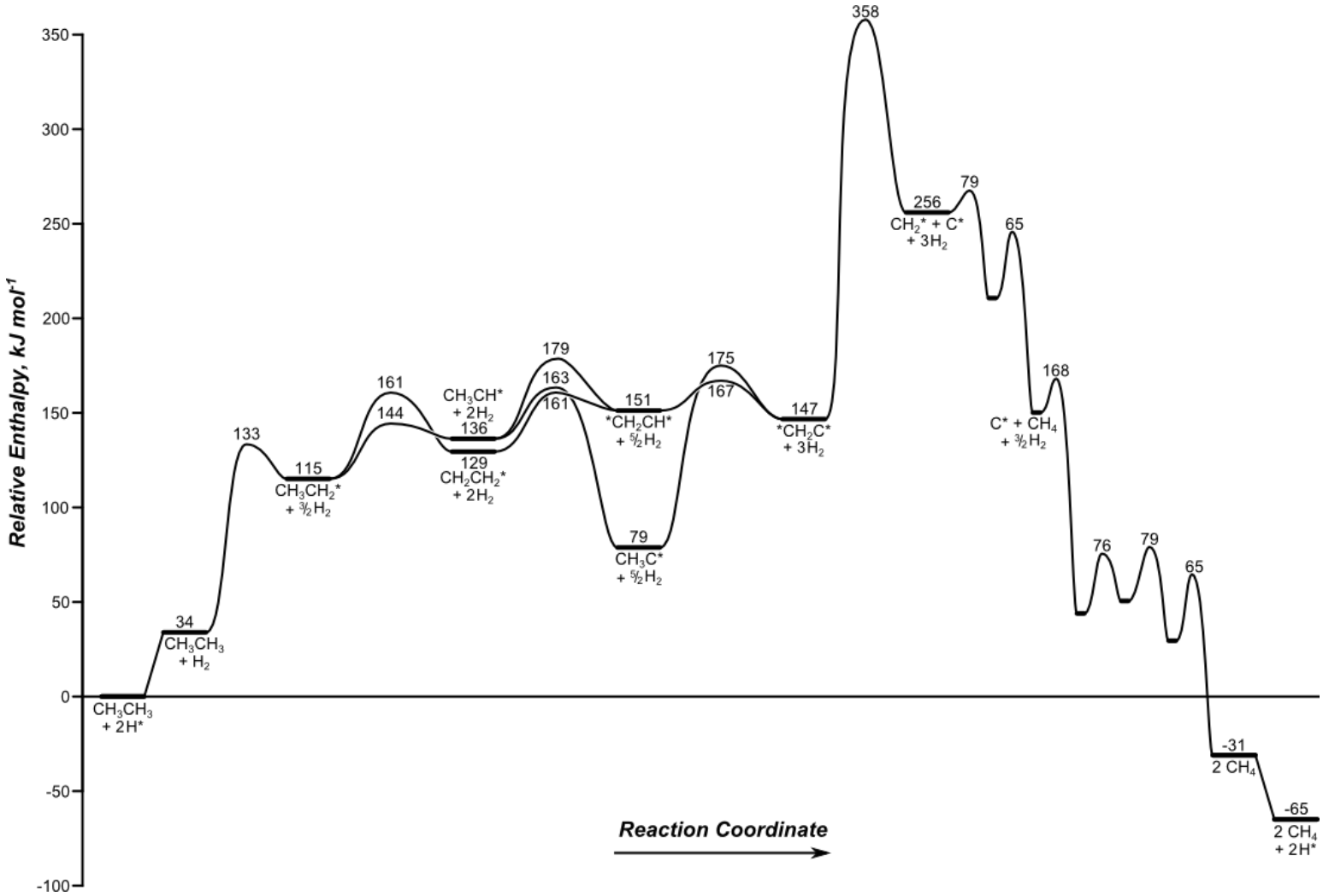

Figure S10. Reaction coordinate diagram for ethane hydrogenolysis via C-C bond rupture in *CH_2C*.

Mechanism I) Ethane Hydrogenolysis via *CHC* Activation:

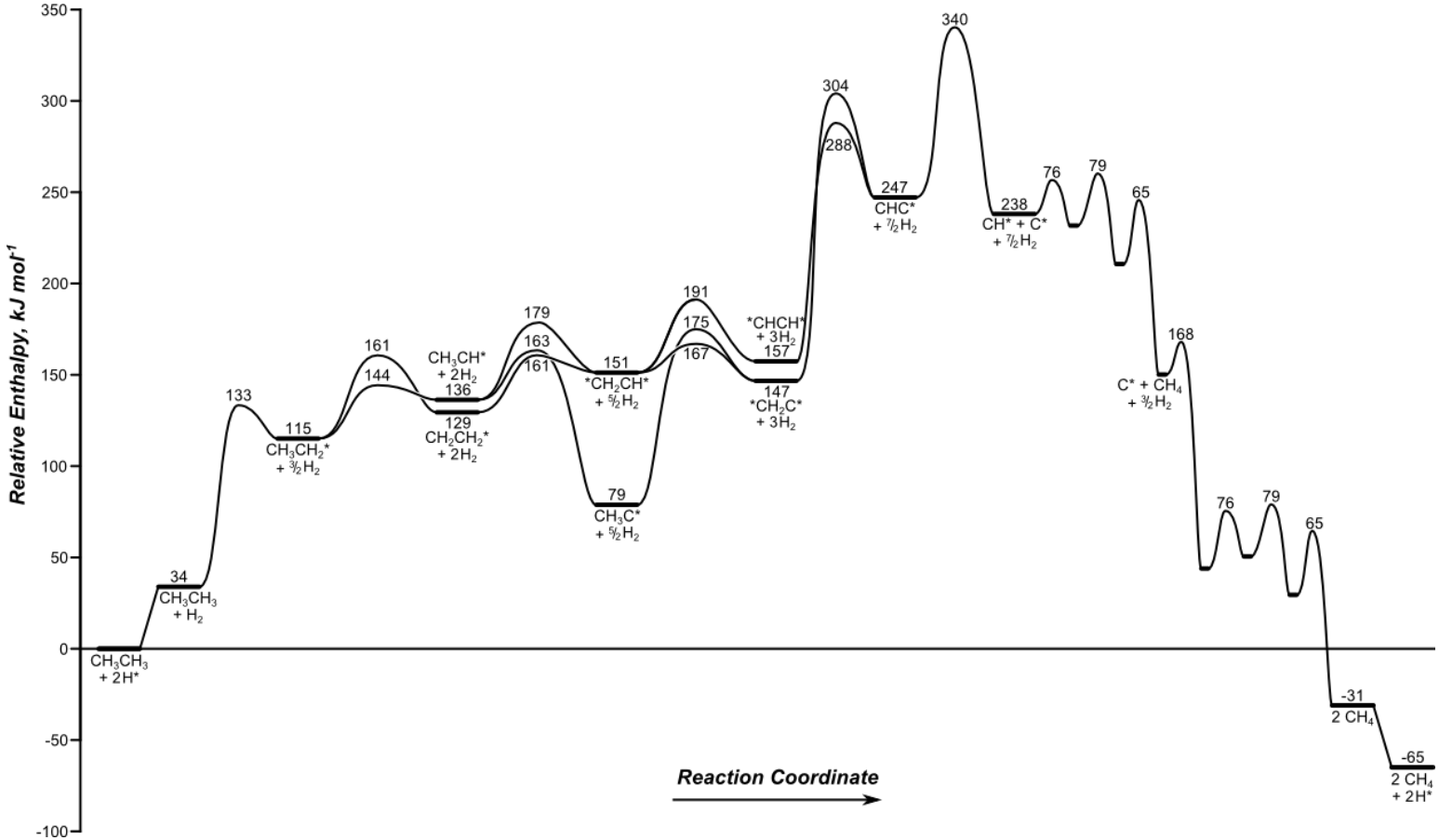

Figure S11. Reaction coordinate diagram for ethane hydrogenolysis via C-C bond rupture in *CHC*.

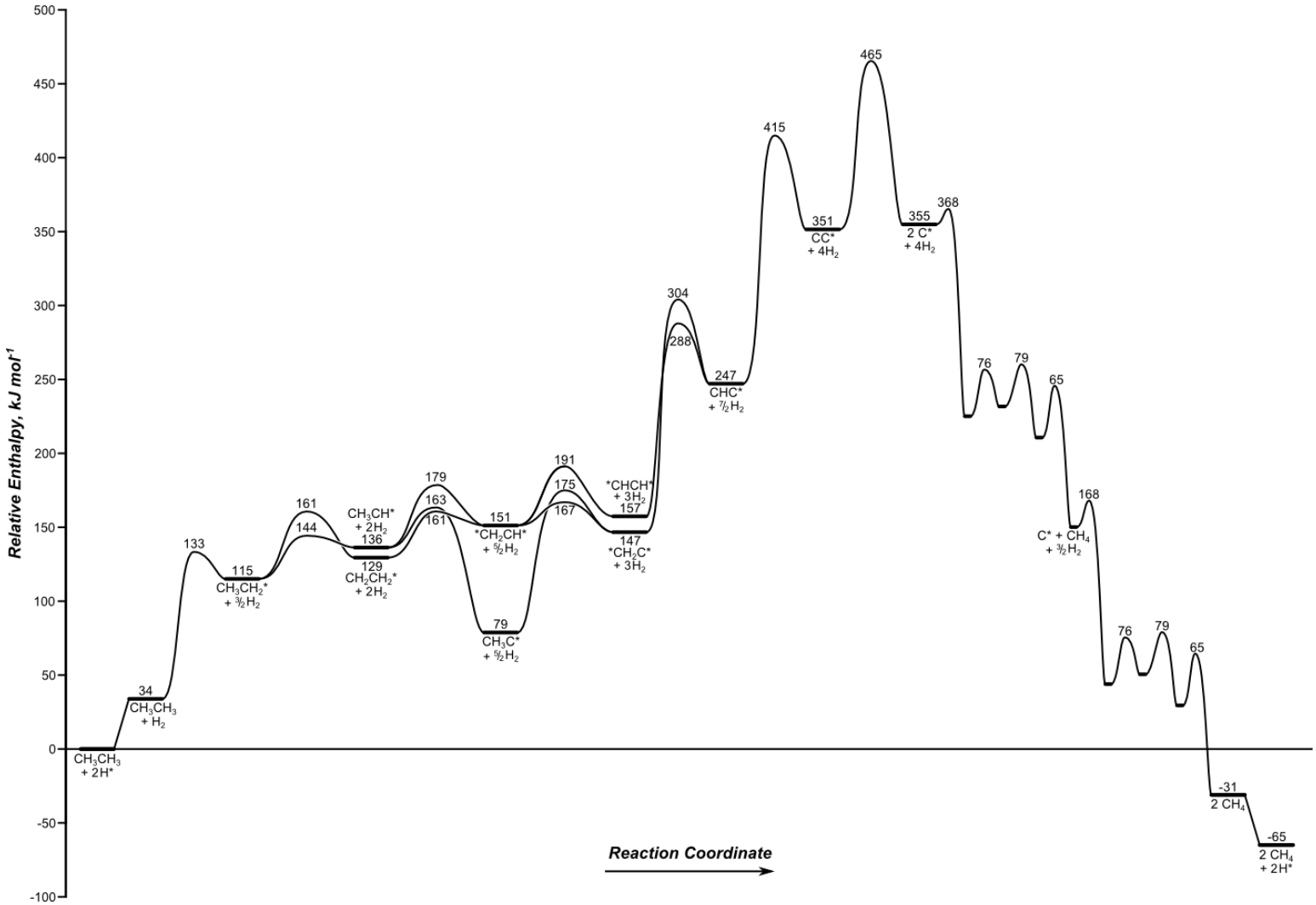

Figure S12. Reaction coordinate diagram for ethane hydrogenolysis via C-C bond rupture in *CC*.